Investigation of the in vitro genotoxicity of two rutile TiO 2 nanomaterials in human intestinal and hepatic cells and evaluation of their interference with toxicity assays

Pégah Jalili, Nelly Gueniche, Rachelle Lanceleur, Agnès Burel, Marie-Thérèse Lavault, Holger Sieg, Linda Böhmert, Thomas Meyer, Benjamin-Christoph Krause, Alfonso Lampen, et al.

INVESTIGATION OF THE *IN VITRO* GENOTOXICITY OF TWO RUTILE TiO_2 NANOMATERIALS IN HUMAN INTESTINAL AND HEPATIC CELLS AND EVALUATION OF THEIR INTERFERENCE WITH TOXICITY ASSAYS

Pégah JALILI[1], Nelly GUENICHE[1], Rachelle LANCELEUR[1], Agnès BUREL[2], Marie-Thérèse LAVAULT[2], Holger SIEG[3], Linda BOEHMERT[3], Thomas MEYER[4], Benjamin-Christoph KRAUSE[5], Alfonso LAMPEN[3], Irina ESTRELA-LOPIS[4], Peter LAUX[5], Andreas LUCH[5], Kevin HOGEVEEN[1,6] and Valérie FESSARD[1]

[1]ANSES, French Agency for Food, Environmental and Occupational Health & Safety, Fougères Laboratory, Toxicology of Contaminants Unit, 10 B rue Claude Bourgelat, 35306 Fougères, France

[2]MRic Cell Imaging Platform, BIOSIT, University of Rennes 1, Campus Santé de Villejean, 2 avenue du Pr Léon Bernard - CS 34317, 35043 Rennes, France

[3]Federal Institute for Risk Assessment (BfR), Department of Food and Safety, Max-Dohrn-Straße 8-10, 10589 Berlin, Germany

[4]Institute of Medical Physics & Biophysics, Leipzig University, Härtelstraße 16, 04107 Leipzig, Germany

[5]Federal Institute for Risk Assessment (BfR), Department of Chemical and Product Safety, Max-Dohrn-Straße 8-10, 10589 Berlin, Germany

[6]ASPIC Cellular Imaging Platform, 10 B rue Claude Bourgelat, 35306 Fougères, France

Corresponding author:

Valerie FESSARD

Anses Laboratoire de Fougères

Unité de Toxicologie des contaminants

10 B rue Claude Bourgelat – Javené CS 40608,

35306 Fougères, FRANCE

Tel: +33 (0)2 99 17 78 67

Fax: +33 (0)2.99.94.78.80

E-mail: Valerie.fessard@anses.fr

ABSTRACT

TiO_2 nanomaterials (NM) have a wide range of industrial applications, including their use in food products. The incorporation of these NMs in consumer products represents a clear concern for public health safety agencies and consumers, and further investigation of the potential impact of these products on human health is necessary. Indeed, since human oral exposure to TiO_2 NMs is expected to increase in the years to come, there exist legitimate concerns about the risk assessment of these nanomaterials present in food products. A considerable amount of studies investigating the adverse effects of TiO_2 NMs have focused on the genotoxic effects of these NMs, and more recently they have been classified by the International Agency for Research on Cancer (IARC) as carcinogen group 2B following inhalation studies (IARC 2010). While numerous data are available for anatase or mixes of anatase/rutile forms, the toxicity and the genotoxicity of rutile TiO_2 NMs have been rarely investigated. The aim of our study was therefore to investigate the cytotoxic and genotoxic effects of two rutile TiO_2 NMs, differing in surface coating, NM103 (hydrophobic) and NM104 (hydrophilic), on intestinal and hepatic cell models. Following 3 or 24 h treatments with concentrations of TiO_2 NMs from 1.2 to 80 µg/cm^2, we have assessed the genotoxicity of these NMs with γH2AX, alkaline comet assay and micronucleus (MN) assays. Cellular viability and effects on oxidative stress were also evaluated. Although TEM imaging demonstrated the presence of the two TiO_2 NMs within the cytoplasm, no significant cytotoxic or genotoxic were observed in either cell model. We have also evaluated and taken into account a variety of potential sources of interference of NMs with cellular assays. TiO_2 NMs present in the cytoplasm introduce uncertainty in the scoring of micronuclei, and therefore this assay is not recommended for the evaluation of the genotoxicity of TiO_2 NMs, or other NMs demonstrating similar interference. The unique properties of TiO_2 NMs introduce additional complexity for genotoxicity testing, and caution must be taken in order to obtain reliable results necessary for accurate hazard assessment.

Keywords: *In vitro*, genotoxicity, titanium dioxide nanomaterials, rutile, interference

1 INTRODUCTION

TiO_2 NMs are commonly used in industrial applications and are present in a wide range of consumer products including food products. The use of TiO_2 NMs in the food industry includes applications as white color additive, flavor and opacity enhancer which can be found in candies, dairy products, dried vegetables, nuts, seed, soup, various processed foods, dietary supplements as well as in beer and wine (Peters et al. 2014, Lim et al. 2015, EFSA 2016). Due to their antimicrobial properties, they are also used as coating for plastic packaging (Chaudhry et al. 2008, Youssef et al. 2015). In addition, due to their photo-catalytical properties, TiO_2 NMs can also be used in the degradation of pollutants in water treatment plants (Theron et al. 2008, Chong et al. 2010).

Based on the assumption that food grade TiO_2 (E171) contains a mean of 36% of nanosized particles, it was estimated that the oral exposition of adults in the United States is around 0.1 mg nanoscale TiO_2/kg bw/day, and is 2-4 time higher for children (Weir et al. 2012). More recently, the European Food Safety Authority (EFSA) collected a complete European database on human dietary exposure to TiO_2 NMs. For the maximum level exposure assessment scenario, the mean exposure estimates ranged from 0.4 mg/kg bw per day for infants and the elderly, to 10.4 mg/kg bw per day for children (EFSA 2016). Nevertheless, a health-based guidance value for food grade TiO_2 has not been established.

Most of the studies investigating TiO_2 NMs have addressed their adverse effects upon exposure by inhalation. However, more recent studies have investigated the impact of TiO_2 following oral exposure, including the translocation across the intestinal barrier (Cabellos et al 2017; Brun et al. 2014), the modifications due to the food matrix and the gastrointestinal tract (McClements et al. 2016), the effect on gut microbiota (Chen et al. 2017; Dudefoi et al. 2017), as well as on the effects of TiO_2 NMs on nutrient absorption (Guo et al. 2017). According to chronic inhalation studies, TiO_2 has been classified by the International Agency for Research on Cancer (IARC) (IARC 2010) as Group 2B carcinogen “possibly carcinogenic to humans”, and France has recently submitted a CLH (Harmonised Classification and Labeling) report for carcinogenic endpoint according to the CLP (Classification Labelling Packaging) regulation 1272/2008/EC in 2015 (Regulation (ec) no 1272/2008 of the european parliament and of the council 2008). Recently, a promoter effect of TiO_2 in the colon of rats

after 100 days of exposure has been observed (Bettini et al. 2017) and the French agency for food, occupational and environmental health and safety (ANSES) recommended further testing in order to adequately evaluate the carcinogenic properties of TiO_2 through oral exposure (ANSES 2017).

The genotoxic effects of TiO_2 NMs *in vivo* following oral exposure have been studied primarily in bone marrow and liver (Trouiller et al. 2009, Sycheva et al. 2011, Chen et al. 2014, Grissa et al. 2015, Donner et al. 2016). Contradictory results have been obtained from comet and micronucleus assays from these studies. As bone marrow is not a likely target tissue of TiO_2 NMs following oral administration, the relevance of the bone marrow micronucleus assay for the evaluation of the genotoxicity of NMs remains debatable (Donner et al. 2016).

Although numerous *in vitro* studies looking at the genotoxicity of TiO_2 NMs have been performed, there exists no clear consensus concerning the genotoxicity of these NMs. In the majority of studies, genotoxic effects of nanosized TiO_2 were observed with anatase or mixtures of anatase/rutile particles (Petkovic et al. 2011, Fisichella et al. 2012, Gerloff et al. 2012, Prasad et al. 2013, Kermanizadeh et al. 2014, Shukla et al. 2014, Zijno et al. 2015, Dorier et al. 2017, El Yamani et al. 2017). Although only few studies have been performed with rutile forms, some reported genotoxic effects in human hepatoblastoma C3A cells (Kermanizadeh et al. 2012), human primary peripheral lymphocytes (Tavares et al. 2014), human amniotic epithelial WISH cells (Saquib et al. 2012), human bronchial epithelial 16-HBE cells (Ghosh et al. 2017) and Balb/3T3 mouse fibroblasts (Uboldi et al. 2016). Moreover, differences in the genotoxic potential of rutile TiO_2 NMs have been reported to be due to surface coating (Kermanizadeh et al. 2012). In the present study, the genotoxicity of two similar-sized rutile TiO_2 NMs differing in their surface coating (NM103 hydrophobic and NM104 hydrophilic) has been investigated using several genotoxicity endpoints: alkaline and Fpg-modified comet assays to detect DNA breaks including oxidative lesions, gamma-histone H2AX (γH2AX) as marker of DNA double strand breaks and the micronucleus assay to detect chromosomal mutations. Pertinent cell models relevant to human oral exposition scenarios have been used: the human intestinal Caco-2 cell line, as well as the human hepatocyte cell line HepaRG, since some studies have reported that TiO_2 NMs are capable of crossing the intestinal barrier and accumulate in liver (Wang et al. 2007, Cui et al. 2011, Heringa et al. 2016).

Additionally, numerous publications have demonstrated the interference of TiO_2 NMs in a wide range of biological assays, which may then lead to false-positive or false-negative results (Azqueta et al. 2015, Di Bucchianico et al. 2016, Ferraro et al. 2016, Bessa et al. 2017, Li et al. 2017). In the current study, we have therefore described and taken into account various sources of interference within our assays.

2 MATERIAL AND METHODS

2.1 Chemicals

Dimethylsulfoxide (DMSO), Bovine serum albumin (BSA), insulin, cytochalasin B, formamidopyrimidine-DNA glycosylase (Fpg) and Neutral Red Solution (0.33%) were purchased from Sigma (St. Quentin-Fallavier, France). Methylmethanesulfonate (MMS) was supplied by Acros Organics (Fairlawn, NJ). Williams' E medium, Fetal Bovine Serum fetalclone II (FBS), penicillin and streptomycin were purchased from Invitrogen Corporation (Illkirch, France). Hydrocortisone hemisuccinate was from Upjohn Pharmacia (Guyancourt, France). Hyclone™ DMEM/high glucose was obtained from GE Healthcare Life Science (Logan, UT, USA) and fetal bovine serum for Caco-2 cells from Capricorn scientific (Ebsdorfergrund, Germany).

2.2 Nanomaterials and dispersion

The selected TiO_2 NMs NM103 (rutile-hydrophobic-25nm) and NM104 (rutile-hydrophilic-25nm) were obtained from the European Commission Joint Research Centre, Institute for Health and Consumer Protection (JRC-IHCP, Ispra, Italy). NM characteristics given by suppliers are provided in table 1.

The NANOGENOTOX protocol was used for nanomaterial dispersion (Hartmann et al. 2015). Briefly, particle powder was pre-wetted in absolute ethanol (0.5 % of the final volume) in a scintillation vial and dispersed at a concentration of 2.56 mg/mL in 0.05% BSA in ultra-pure water by sonication in ice for 16 min at 400W using a Branson ultrasonic sonicator with a 13 mm probe diameter.

2.3 Physicochemical characterization

A thorough characterization of NM103 and NM104 is available in the JRC report (Rasmussen et al. 2014), and has been performed in different media in numerous European projects including NANOGENOTOX and NANoREG.

The hydrodynamic diameter of TiO_2 NMs was characterized by Dynamic Light Scattering (DLS) and NanoTracking Analysis (NTA) according to protocols that have been developed previously at ULEI and BfR based on the NANoREG project (NANoREG 2016).

The DLS measurements were performed using a Brookhaven Omni zetaPALS instrument equipped with a 659 nm laser diode. The scattered light was detected using a 90° experimental set-up. The NM size and the polydispersity index (PDI) were measured immediately after preparation and checked after 24 h to verify the stability of the particle dispersion. The particle size was determined in dispersion stock solution (ultra-pure water with 0.05 % BSA) as well as under cell culture conditions (DMEM +10% FBS, and William's Medium +5% FBS) at 100 µg/ml. The samples were allowed to equilibrate at room temperature for at least 5 minutes before measurement. For each sample, five repeated measurements were performed and at least 3 independent preparations were assessed. Z-average cumulant analysis was performed by ZetaPALS Particle Sizing Software 5.31. For comparison, a second set of measurements was performed with a Malvern Nano ZS (Malvern Instruments, Malvern, UK) equipped with a 633 nm laser diode and with the detection of the scattered light using a 173° set-up. With this equipment, one dispersion for each NM was performed; 3 independent dilutions were performed with 6 replicates and 10 DLS measurements each. Measurement of the zeta potential of NM103 and NM104 was performed using a Malvern Nano ZS (Malvern Instruments, Malvern, UK).

The particle size was also measured using the NanoSight LM10 system (NanoSight Ltd, Amesbury, UK), configured with a 532 nm laser and a high sensitivity digital camera system (OrcaFlash2.8, Hamamatsu C11440, NanoSight Ltd). Videos were collected and analyzed using the NTA-software (version 2.3). Temperature was fixed at 25°C. Each sample was diluted in ultra-pure water so that the concentration was between 2×10^8 and 9×10^8 particles/ml. For each sample, at least

five positions were recorded, generating six replicate histograms which were finally merged. At least three independent measurements were performed.

2.4 Cell culture and treatment

The human colorectal adenocarcinoma Caco-2 cell line was obtained from the European Collection of Authenticated Cell Cultures (ECACC 86010202). Caco-2 cells (passages 25–38) were cultured in 75 cm^2 flasks (Corning Inc. Life Sciences) in DMEM supplemented with 10% FBS, 50 U/ml penicillin and 50 µg/ml streptomycin and maintained at 37°C under an atmosphere of 5% CO_2. Cells were seeded at 14,285 cells/cm^2 either in 96 well plates (High content analysis, glutathione level and neutral red uptake), 6 well plates (micronucleus assay), 24 well plates (comet assay) or in 35 mm Petri dishes (TEM). Differentiated Caco-2 cells were obtained after 21 days in culture.

HepaRG cells were cultured as previously described (Aninat et al. 2006) in William's E medium supplemented with 10% FBS, 100 U/ml penicillin, 100 µg/ml streptomycin, 2 mM glutamine, 5 µg/ml insulin and 50 µM hydrocortisone hemisuccinate. Briefly, HepaRG cells (passages 13–19) were seeded at a density of 26,000 cells/cm^2 either in 96 well-plates (High content analysis, glutathione level and neutral red uptake), 12 well plates (micronucleus assay), 24 well plates (comet assay) or in 35 mm Petri dishes (TEM). After 2 weeks in culture, cell differentiation was induced by adding 1.7 % DMSO to the culture medium for 2 additional weeks (differentiation medium).

Differentiated Caco-2 and HepaRG cells were treated for 3 or 24h with TiO_2 NMs (NM103 or NM104) at concentrations of 1.25 to 80 µg/cm^2 in DMEM + 10% FBS and William's medium + 5% FBS respectively. Equivalence between µg/ml and µg/cm^2 are shown in Table 2.

2.5 Uptake and localization in cells by transmission electron microscopy (TEM)

Following a 24 h treatment with NMs, cells were rinsed twice with Phosphate-buffered saline (PBS) and with 0.15 M Na cacodylate buffer (pH 7.2) before fixation by drop wise addition of glutaraldehyde (2.5%) for 45 min. The cells were rinsed several times with 0.15 M Na cacodylate buffer and post fixed with 1% osmium tetroxide for 45 min. After further rinsing with cacodylate buffer, the samples were dehydrated through an ethanol gradient from 70% to 100% and infiltrated in

a mixture of acetone-epon resin (50/50) for 3 h, then, in pure epon resin for 16 h. Finally, the samples were embedded in DMP30-epon for 24 h at 60°C. Ultra-thin sections (90 nm) were cut on a Leica UC7 ultracut, collected onto copper grids and double-stained with 4% uranyl acetate then with lead citrate (Reynold solution). Examination was performed with JEOL 1400 electron microscope operated at 120 kV equipped with a 2k-2k camera from Gatan (Orius 1000).

2.6 Neutral Red (NR) uptake assay

Following a 24 h treatment with TiO_2 NMs, the cells were washed twice with PBS and incubated at 37°C for 2 h with 100 µl of 33 µg/ml Neutral Red solution prepared in PBS. The cells were then washed 2 times with PBS and 100 µl/well of NR extraction solution (1% (v/v), acetic acid (Sigma Aldrich) and 50% (v/v) ethanol (Merck Millipore) in ultra-pure water) was added to solubilize the lysosomal neutral red. The plates were gently shaken for 5 minutes and the absorbance was recorded with a FLUOstar Optima microplate reader (BMG Labtek, Champigny sur Marne, France) at 540 nm.

In order to account for interference with the assay due to the absorbance of TiO_2 NMs at 540 nm (Appendix fig 1), control wells for each nanoparticle concentration were treated as previously described except that they were incubated with PBS in the place of NR for 2 h. Mean optical density (OD) values from treated cells incubated without NR were substracted from mean OD values from treated cells incubated with NR ($OD^{NMs} = OD^{cells+NMs\ with\ NR} – OD^{\ cell+NMs}$ and $OD^{Control} = OD^{cells\ control\ +\ with\ NR} – OD^{\ cell\ control}$). Cellular viability was calculated by $OD = (OD^{NMs} / OD^{control}) \times 100$**.** Three independent experiments were performed.

2.7 Reduced glutathione (GSH) levels

After a 24 h treatment with NMs, cells were washed two times with PBS and incubated with 100 µl freshly prepared monochlorobimane (mBCl) solution (40 µM mBCl in PBS) for 20 min. After another washing step, cells were incubated with mBCl desorption solution (0.7 % sodium dodecyl sulfate w/v in isopropanol) at room temperature on a shaker for 30 min. Fluorescence was measured in a Tecan fluorescence plate reader at 460 nm. As a positive control, a 100 µM buthioninesulfoximine (BSO) solution was used. Three independent experiments were performed.

2.8 Fluorescent staining and High Content Analysis (HCA)

Interference of NMs with HCA assays was assessed by comparing the staining of HepaRG cells treated with the highest concentration of NM103 and NM104 (80 µg/cm^2) with DAPI (4',6-diamidino-2-phenylindole), DAPI + secondary Ab and DAPI + primary and secondary Ab. The fluorescence intensity at 650 nm was measured and expressed as fold increase compared to control cells. Two independent experiments were performed (Appendix fig 2). No interference with TiO_2 NMs was observed at this wavelength.

2.8.1 CellROX

Prior to treatment, cells were incubated 1h with 5 µM CellROX Deep Red Reagent (Thermo Scientific, Paisley, UK) diluted in serum-free DMEM. After 3 hours of treatment with TiO_2 NMs, cells were washed two times with PBS and incubated with 3 µg/ml Hoechst in DMEM supplemented with 10 % FBS for 30 min before scanning with an ArrayScan VTI HCS Reader (Thermo Scientific, Waltham, USA). Images were analyzed using the Target Activation module of the BioApplication software. For each well, 10 fields (20 × magnification) were scanned and analyzed for fluorescence quantification of reactive oxygen species (ROS) at 647 nm. Three independent experiments were performed.

2.8.2 γH2AX immunofluorescence

After treatment with NMs for 3 h or 24 h, cells were fixed 10 min with 4% formaldehyde in PBS and permeabilized with 0.2% Triton X-100. Plates were then incubated in blocking solution (PBS with 1% BSA and 0.05% Tween-20) for 30 min before addition of primary antibodies. All antibodies were prepared in blocking solution. The primary and secondary antibodies were purchased from Abcam (Cambridge, UK): mouse monoclonal anti γH2AX ser139 (ab26350), and goat anti-mouse IgG H&L AlexaFluor 647 (ab150115). Primary antibodies (1/1000) were incubated overnight at 4°C. After washing with PBS + 0.05% Tween-20, secondary antibodies (1/1000) were incubated for 45 min at

room temperature. Nuclei were stained with DAPI (1 μg/ml in PBS) for 5 min for automated cell identification by high content analysis.

Plates were scanned with an ArrayScan VTI HCS Reader (Thermo Scientific, Waltham, USA) and analyzed using the Target Activation module of the BioApplication software. For each well, 10 fields (10× magnification) were scanned and analyzed for immunofluorescence quantification at 647 nm. Cytotoxicity was determined by cell counts from DAPI staining and was expressed as percentage of cells compared to control cells. γH2AX was quantified in cell nuclei and expressed as fold increase compared to control cells. Three to five independent experiments were performed.

2.9 Comet assay

After a 3 (Appendix fig 3) or 24 h treatment with NMs, cells were trypsinized, centrifuged (2 min, 136 g), and the alkaline comet assay (migration of 24 min, 0.24 V/cm and 300 mA) was performed as described in previous studies (Josse et al. 2008, Le Hegarat et al. 2012). DNA was stained with propidium iodide (2.5 μg/ml in PBS) immediately prior to blind scoring with a fluorescence microscope (Leica DMR) equipped with a CCD-200E camera. For each experiment, at least 100 cells per concentration were analyzed using the Comet Assay IV software (Perceptive Instruments, Haverhill, UK). Both tail length and tail intensity were evaluated in order to identify which parameter may be more suitable, as suggested by George et al 2017. When DNA damage was too high to score, the cells were counted as hedgehogs.

To determine the level of oxidized bases, a modified comet assay, using bacterial DNA repair enzymes can be performed (Collins et al. 1993). Among these enzymes, formamidopyrimidine-DNA glycosylase (Fpg) catalyzes excision of oxidized purines including the major purine oxidation product 8-oxoguanine, into single-strand breaks detectable by the comet assay (Dusïnská et al. 1996). All preparative steps were conducted according to the protocol described above, with additional steps: after lysis the slides were washed two times for 5 min with enzyme buffer (0.1 M KCl, 0.2 mM EDTA, 40 mM 4-(2-Hydroxyethyl)piperazine-1-ethanesulfonic acid, N-(2-Hydroxyethyl)piperazine-N′-(2-ethanesulfonic acid) (HEPES), 0.2 mg/ml BSA). Slides were then incubated with enzyme buffer (control slide) or with 9 U Fpg /slide at 37°C for 30 min. The slides were then processed as described

previously. Methyl methanesulfonate (MMS) was used as positive control. Four independent experiments were conducted.

2.10 Particle interaction with the comet assay

To evaluate the interaction of particles with the comet assay in terms of DNA migration, the protocol of Bessa et al (2017) (Bessa et al. 2017) was adapted. Briefly, NM103 or NM104 TiO_2 NMs were mixed with low-melting point agarose (LMP) at final concentrations of 28 and 128 µg/ml corresponding to cell treatment conditions of 7.5 and 33.7µg/cm^2. After 24 h exposure to 2.5 µg/ml of MMS (genotoxic reference), cells were trypsinized and centrifuged (2 min, 136 g). The cell pellet was then recovered with the LMP/NM mix, loaded on pre-coated slides to further process in the alkaline comet assay as previously described, without using Fpg (Appendix fig 4.B). The results obtained were compared with a negative control (cells treated with MMS, recovered with LMP in the absence of NMs). Two independent experiments were conducted.

2.11 Cytokinesis-block micronucleus assay (CBMN)

The CBMN assay was performed according to guideline 487 from the Organization for Economic Co-operation and Development (OECD, 2008). MMS was used as positive control. Following a 24 h treatment, two washing with PBS and a trypsinization step, Caco-2 cells were seeded in 12 well-plate at 42,000 cells/cm^2 and HepaRG were seeded at 15,000 cells/cm^2 in Lab-Tek II chamber slide system®. After 48 h (for Caco-2 cells) or 24 h (for HepaRG cells), the medium was replaced with media containing 4.5 µg/ml cytochalasin B. Following 28 h (for Caco-2 cells) or 24 h (for HepaRG cells), cytochalasin was removed and a 1.5 h recovery step in medium with 10% FBS was performed.

Caco-2 cells were trypsinized and centrifuged for 5 min at 136 g. After a quick hypotonic shock in 0.075 M potassium chloride at 37 °C, the cells were centrifuged again and fixed with a mixture of methanol/acetic acid 3:1 (v/v) diluted 1:1 in medium with 10% FBS (5 min), and then fixed for an additional 15 minutes at room temperature with undiluted methanol/acetic acid 3:1 (v/v). The cells were then centrifuged for 5 min at 136 g and kept overnight at 4°C. Cells were spread onto cold microscope slides kept in 50% ethanol.

After recovery, HepaRG cells were fixed 10 min with 4% formaldehyde, rinsed two times with PBS, and permeabilized with 0.5 % Triton X-100 for 5 min.

The slides were stained with acridine orange (100 µg/ml) and observed with a Leica fluorescence microscope at 40 × magnification. Three independent experiments were performed. For each experiment, at least 1000 binucleated cells were scored per culture, with two cultures per condition. The number of mononucleated (MN), binucleated (BN) and polynucleated cells (POL) were recorded as well as the number of mononucleated (MNMN) and binucleated cells (BNMN) with micronuclei. The replication index (RI) was calculated using the formula of the OECD guideline 487.

2.12 Statistics

Results from cell cultures subjected to different treatment conditions were tested for statistical significance using one-way Analysis of variance (ANOVA) followed by Dunnett's post hoc tests using GraphPad Prism 5. All error bars denote SEM. Statistical significance was depicted as follows: $p < 0.1$, $*p < 0.05$, $**p < 0.01$, $***p < 0.001$.

For the micronucleus assay, the percentages of BNMN cells in treated cells and control cells were compared using the one-way Pearson chi-square test. Treatment means were considered significantly different at $p < 0.05$.

3 RESULTS

3.1 Particle characterization

DLS and NTA methods were applied to analyze particle size and stability in the stock dispersion solutions as well as in cell media (DMEM and William's with supplements and serum) immediately after addition (0 h) and after 24 h (Table 3).

For all conditions following NM dispersion, the PDI was > 0.1 indicating a polydisperse size distribution of TiO_2 NMs in the stock dispersion solution and in media.

DLS analysis of NMs in the stock dispersion solution revealed a different mean agglomerate size of 611 ± 185 nm for NM103 and 370 ± 66 nm for NM104 which increased after 24 h to 820 ± 250 and

528 ± 124 nm respectively. This variation over time demonstrated the instability of NM103 and NM104 TiO_2 NMs in term of agglomeration in the stock dispersion solution. Such instability over time was not observed when DLS measurements were performed with a Malvern Nano ZS (Appendix table 1). This difference may be attributed to a different measurement angle of the two devices used. Indeed, our data set with the Brookhaven DLS was achieved with an angle of 90°, while the experiment with Malvern DLS was carried out under backscattering conditions at 173°.

In cell culture media, similar mean agglomerate sizes were observed for TiO_2 NM103 (267 ± 8 nm) and NM104 (237 ± 6 nm) in DMEM medium as well as in William's medium (270 ± 10 nm for NM103 and 235 ± 4 nm for NM104 nm) which remained similar after 24 h (Table 3).

The NM size calculated by NTA in the stock dispersion solution was similar for the two TiO_2 NMs immediately following dispersion as well as over time (from 135 to 162 nm)**.** In media, NM agglomerate size was also similar for the two TiO_2 NMs (from 113 ± 6 nm and 122 ± 8 nm at 0 h) and over time (Table 3).

No difference in zeta potential was observed between NM103 and NM104 either in the stock dispersion solution (-23.4 ± 2 for NM103 and -24.3 ± 0.6 for NM104 at 0 h) or in media (-15.7 ± 0.8 for NM103 and -15.8 ± 0.6 for NM104 in DMEM). Zeta potentials of NM103 and NM104 were slightly higher in cell culture media when compared to the stock dispersion solution (Table 3).

3.2 Uptake

Uptake of TiO_2 NMs into cells, as well as the cellular distribution of NMs following uptake, was investigated by TEM after a 24 h treatment (Fig 1). The two TiO_2 NMs were observed inside Caco-2 and HepaRG cells even at the lowest concentration (7.5 µg/cm^2). NM agglomerates of different sizes were seen free or in vesicles, but also in vacuole-like compartments in HepaRG cells, particularly at the highest concentration (Fig 1 G and 1 I). While sometimes localized in close proximity to the nuclear membrane, no NMs were observed inside the nucleus (Fig 1 B). No significant difference in cellular uptake or intracellular distribution was observed between NM103 and NM104 in either cell line.

3.3 Cytotoxicity

The NRU assay was used to measure cytotoxicity in cells exposed to NM103 and NM104 for 24 h (Fig 2A and 2B). The presence of NMs in the culture media was associated with interference due to the absorption of TiO_2 NMs at wavelengths used for NRU quantification, as reflected by concentration dependent increases in the absorbance values in the presence of NMs (Appendix fig 1). Taking into account this interference, no significant effect on cellular viability was observed in the two cell lines with either NM up to concentrations of 80 µg/cm^2.

Direct cell counts obtained from HCA data confirmed the absence of cytotoxicity for both NM103 and NM104 up to 80 µg/cm^2 in the two cell lines (Fig 2C and 2D).

3.4 Oxidative stress

No significant change in reduced glutathione levels was observed in either cell line after a 24 h treatment with either NM103 or NM104 (Fig 3A and 3B).

Investigation of the formation of ROS after 3 h treatment to NMs (Fig 3C and 3D) showed no modification in ROS levels in either cell line following treatment with the TiO_2 NMs.

3.5 Genotoxicity

3.5.1 γH2AX

In both Caco-2 and HepaRG cells, no significant change in γH2AX levels was detected in the nuclei of cells exposed for 3 h or 24 h to NM103 and NM104 up to 80 µg/cm^2 compared to negative controls (Fig 4).

3.5.2 Comet assay

The potential interference of NMs with the alkaline comet assay, including alterations of DNA migration during electrophoresis, either by inducing breaks into the naked DNA or inhibiting DNA migration, was assessed (Fig 5) according to the protocol proposed by Bessa et al (2017) (Bessa et al. 2017). No significant modification of DNA damage or migration was observed for either NM103 or

NM104 NMs when Caco-2 cells treated 24 h with 2.5 µg/ml MMS were mixed with LMP agarose and NMs before deposition on pre-coated slides.

The effect of NM103 and NM104 TiO_2 NMs on DNA damage was investigated by the alkaline comet assay in Caco-2 and HepaRG cells after a 3 h (Appendix fig 3) or 24 h (Fig 6) treatment (Fpg-). Oxidative DNA damage was also determined using a modified comet assay with Fpg enzyme (Fpg+). For both Fpg- and Fpg+ conditions, compared to untreated cells, no significant changes in DNA damage were observed either in tail intensity or in tail length following treatment with NM103 and NM104 in Caco-2 and HepaRG cells.

3.5.3 Micronucleus assay

In order to evaluate chromosomal and genomic mutations, the CBMN assay was performed with NM103 and NM104 (Table 4). No significant changes in the percentage of BNMN, MNMN or POL were observed in either Caco-2 or HepaRG cells following a 24 h treatment with NM103 and NM104, compared to negative controls. However, the presence of NMs in cells compromised the proper visualization and scoring of micronuclei when stained with Giemsa or with acridine orange (Appendix fig 5). The scoring of MN could therefore be underestimated with increasing concentrations of NMs, and the absence of response should be taken with caution.

4 DISCUSSION

Many recent studies have addressed the genotoxicity of TiO_2 NMs, and have generated contradictory results and conclusions. Since these inconsistencies could relate to variations in physico-chemical characteristics (size, surface coating and charge...), dispersion protocol, cell systems and cell media as well as protocol schedule, the use of well characterized NMs, standardized dispersion methods, and validated genotoxicity tests are crucial to obtain reliable results.

A thorough characterization of NMs is a prerequisite for genotoxicity testing, in particular since the agglomeration status of TiO_2 was previously shown to affect the outcome of the genotoxicity tests

(Magdolenova et al. 2014). In our study, two complementary methods, DLS and NTA, were used to characterize TiO_2 NM suspensions over time. Both methods confirmed the non-homogenous but stable dispersion of TiO_2 NMs over time in cell culture media, while lower stability was observed in the stock dispersion solution. Similar results on the stability of NM103 and NM104 over time in media were previously observed in a study using the same NANOGENOTOX dispersion protocol (Tavares et al. 2014). Comparable average diameters for NM103 and NM104 in both media (DMEM+10% FBS and William's + % 5 FBS) were observed in our study using either DLS or NTA. Indeed, protein from media can influence NM agglomeration (Murdock et al. 2008, Prasad et al. 2013). However, the apparent size NM103 and NM104 may depend on the medium and/or serum used, as demonstrated in a recent study using DLS (Bermejo-Nogales et al. 2017). Interestingly, despite the difference in surface coating of NM103 and NM104, the zeta potentials of these NMs were similar, both in the stock dispersion solution as well as in cell culture media.

In the present study, we have investigated the genotoxic effects of two rutile forms of TiO_2 NMs in differentiated intestinal Caco-2 and hepatic HepaRG cell lines. Although TEM images demonstrated that both TiO_2 NMs were taken up by the two cell lines, no cytotoxic or genotoxic effects were observed. Moreover, despite the different surface coating between NM103 and NM104, we did not detect any differences in cellular effects. Although the hydrophobic/hydrophilic nature of TiO_2 NMs has been demonstrated to influence certain toxicity pathways (Teubl et al. 2015), other studies have demonstrated an absence of acute cytotoxic responses for both NM103 and NM104 in most of the mammalian cell models tested in the European project MARINA (Farcal et al. 2015), as well as in various fish cell lines (Bermejo-Nogales et al. 2017). In fact, the coating may degrade rapidly over the first 24 h depending on the composition of the medium (http://www.oecd.org/officialdocuments/publicdisplaydocumentpdf/?cote=ENV/JM/MONO(2015)14/ANN7&docLanguage=En). Therefore, it can be suspected that the difference of NM103 and NM104 due to their initial coating can be less obvious after some time in the cell medium which may explain the similar results obtained in our study as well as in other projects.

Evaluation of the interference of NMs with the CBMN assay in previous studies has been primarily focused on their effects on cytochalasin-B, which may affect NM endocytosis through prevention of actin-filament formation (Doak et al. 2009). This effect was eliminated by the addition of cytochalasin B after a few hours of treatment with NMs in order to allow cellular uptake of NMs. However, other types of NM interference with the MN assay have been reported in the literature. Interference can occur due to cytoplasmic NM agglomerates/aggregates when high concentrations are used, and in consequence, uncertainty in scoring may lead to false negative results (Corradi et al. 2012, Guichard et al. 2012, Roszak et al. 2013, Shukla et al. 2013, Zijno et al. 2015, Ghosh et al. 2017, Proquin et al. 2017). We therefore suggest that precautions must be considered when interpreting results from the *in vitro* micronucleus assay with TiO_2 NMs or other NMs that display similar properties.

In the present study, we did not observe any induction of chromosomal damage in the micronucleus assay with the two TiO_2 NMs, although an underestimation of micronuclei scoring due to the interference of NMs at higher concentrations cannot be ruled out. Only a few studies have investigated the genotoxic effects of rutile TiO_2 NMs. An increase in micronuclei was reported in human lymphocytes both with NM103 and NM104 (Tavares et al. 2014) as well as in bronchial BEAS 2B cells treated with NM103 (Di Bucchianico et al. 2016). However negative results were obtained in the MN assay with NM103 and NM104 in different cell lines including Caco-2, as reported in the NANOGENOTOX WP5 report (Nanogenotox 2013b) as well as in bronchial epithelial 16HBE cells with NM104 (Ghosh et al. 2017). A recent study has reported genotoxicity in the MN assay in Balb/3T3 mouse fibroblasts treated 24 h with 10 µg/ml of Ru-10, another rutile TiO_2 NM (Uboldi et al. 2016). Inconsistent results are also observed with anatase or anatase/rutile mixtures, with some authors reporting MN formation (Srivastava et al. 2013, Valdiglesias et al. 2013, Prasad et al. 2014, Shukla et al. 2014) while others did not (Jugan et al. 2012, Vales et al. 2015, Zijno et al. 2015, Uboldi et al. 2016, Ghosh et al. 2017). In light of the conflicting data available in the literature from various cell lines, it is not possible to reach a conclusion concerning the genotoxicity of TiO_2 NMs using the micronucleus assay.

No genotoxic effects were observed using the alkaline comet assay in Caco-2 or HepaRG cells following a 24 h treatment with NM103 and NM104. Numerous publications have reported positive genotoxic responses for TiO_2 NMs with the comet assay, although these studies used primarily anatase and anatase/rutile mixtures (Gerloff et al. 2012, Kermanizadeh et al. 2012, Saquib et al. 2012, Prasad et al. 2013, Roszak et al. 2013, Valdiglesias et al. 2013, Shukla et al. 2014, Ursini et al. 2014, Kansara et al. 2015, El Yamani et al. 2017, Stoccoro et al. 2017). Rutile forms of TiO_2 NMs were negative in the comet assay in Syrian Hamster Embryo (SHE) up to 50 µg/cm^2 after a 24 h treatment (Guichard et al. 2012), in human renal HK2 cells (Kermanizadeh et al. 2013), in HepG2 cells (Petkovic et al. 2011), in Caco-2 cells (Dorier et al. 2015) and in V79 fibroblasts (Hamzeh et al. 2013), although other studies have reported induction of DNA damage in the comet assay after 24 h exposure in various cell lines (Jugan et al. 2012, Saquib et al. 2012, Kermanizadeh et al. 2013). Similarly, a genotoxic effect was observed in the comet assay with NM103 and NM104 in human bronchial cells (Di Bucchianico et al. 2016, Ghosh et al. 2017). Although NM103 was positive in Caco-2 cells according to the NANOGENOTOX WP5 report (Nanogenotox 2013b), the genotoxic response was low, the experiment was performed only once and the possible interference with the assay was not tested, which could explain the discrepancy with our results.

TiO_2 NMs have been demonstrated to generate oxidative stress, and the DNA damage observed with TiO_2 NMs could therefore be a result of oxidative lesions (Petkovic et al. 2011, Shukla et al. 2011, Kermanizadeh et al. 2012, Saquib et al. 2012, Shukla et al. 2013, Zijno et al. 2015, Di Bucchianico et al. 2016, El Yamani et al. 2017). Although it is generally suggested that anatase forms are more efficient in producing ROS (Zhang et al. 2013, Zijno et al. 2015), several publications have demonstrated that rutile NMs can be as potent in generating oxidative stress (Jin et al. 2011, Saita et al. 2012, Numano et al. 2014, Sund et al. 2014, Dorier et al. 2015, Sweeney et al. 2015). We therefore conducted a modified comet assay using Fpg, a DNA repair enzyme which recognizes oxidative DNA lesions. In accordance with the results from the classical comet assay, no DNA damage was observed with either NM103 or NM104 following a 24 h treatment. This absence of oxidative DNA damage is consistent with our results demonstrating an absence of effects on GSH levels. Similarly,

Kerminazadeh et al. (2012) did not observe changes in reduced glutathione levels, despite the H2-DCFDA assay demonstrating the production of ROS by rutile TiO_2 NMs (Kermanizadeh et al. 2012). The authors suggested that the liver cell model C3A were sufficiently protected by robust anti-oxidant defense mechanisms in these cells, thereby preventing GSH depletion following TiO_2 exposure.

As oxidative DNA damage can be a punctual effect which can be repaired within the 24 h treatment, a short treatment time is also recommended (Ursini et al. 2014, El Yamani et al. 2017). No increase in DNA damage with the comet assay was observed following 3 h treatment with TiO_2 NMs in our study (Appendix fig 3). This is consistent also with the absence of significant changes in ROS formation.

The overall absence of DNA damage following a 3 h and 24 h treatment with the two rutile TiO_2 NMs was further confirmed by nuclear γH2AX, a marker of DNA double strand breaks. The rare publications which studied γH2AX levels following treatment with anatase forms of TiO_2 NMs also demonstrated negative results (Jugan et al. 2011, Jugan et al. 2012, Valdiglesias et al. 2013).

Our results from a panel of genotoxicity tests suggest an absence of direct interaction of TiO_2 NMs with DNA, which is supported by TEM observation showing exclusion of TiO_2 NMs from the nucleus. In fact, TiO_2 NMs were only rarely observed in cell nuclei following *in vitro* exposure. Such observations have been suggested to arise as a result of their integration during mitosis (Kim et al. 2011, Ahlinder et al. 2013). However, in studies where genotoxic effects were observed using the comet assay following treatment with TiO_2 NMs, the majority of these concluded that the response was due to oxidative stress (Kermanizadeh et al. 2012, Saquib et al. 2012, Zijno et al. 2015, Di Bucchianico et al. 2016). In our study, we have demonstrated that two rutile TiO_2 NMs, NM103 and NM104, did not induce genotoxic effects or oxidative stress. Indeed, no significant changes in ROS formation or γH2AX levels were observed following 3 h or 24 h treatments with TiO_2 NMs.

Our study has evaluated and taken into consideration the potential interference of TiO_2 NMs with biological assays. Several publications have described problems associated with these tests for the evaluation of NM toxicity *in vitro* (Magdolenova et al. 2014, Karlsson et al. 2015, Ferraro et al. 2016, Bessa et al. 2017). In fact, it has been suggested that the presence of NMs during the comet assay can affect migration during electrophoresis by inducing breaks, inhibiting DNA migration, or preventing correct DNA rewinding after electrophoresis. In our study, following the comet assay protocols proposed by Bessa et al (2017) we did not observe any NM interference with DNA migration.

Interference of TiO_2 NMs in the quantification of fluorescence intensity could also introduce uncertainty in the interpretation of results from the comet assay. Indeed, the use of tail length instead of tail intensity has been proposed to avoid potential NM interference with comet scoring (George et al. 2017). By comparing tail length and tail intensity, we did not observe any significant difference between the two scoring methods.

1. CONCLUSION

Two rutile TiO_2 NMs, NM103 and NM104, did not generate acute cytotoxic or genotoxic effects in Caco-2 or HepaRG cells, despite the presence of NMs within the cell. Although the micronucleus test is widely used for the evaluation of the genotoxicity for a wide range of chemical compounds, the large agglomerates/aggregates of TiO_2 NMs present and visible in the cytoplasm introduce uncertainty in the scoring and therefore is not recommended for the evaluation of the genotoxicity of TiO_2 NMs, or other NMs demonstrating similar interference. The comet assay may be more suitable for the genotoxicity testing of NMs, however certain precautions must be taken into consideration in order to generate robust results. Interference of NMs with assays must also be checked when investigating colorimetric measurements as well as fluorescent markers. The unique properties of NMs that render them attractive for industrial applications may also raise issues that complicate their evaluation. Our

results confirm that interference of NMs with toxicity and genotoxicity testing must be taken into account in order to generate reliable results which can be considered for hazard assessment.

DECLARATION OF INTEREST

The authors declare that there are no conflicts of interest.

FUNDING INFORMATION

This publication arises from the French-German bilateral project SolNanoTOX funded by the German Research Foundation (DFG, Project ID: DFG (FKZ LA 3411/1-1 respectively LA 1177/9-1) and the French National Research Agency (ANR, Project ID: ANR-13-IS10-0005).

ACKNOWLEDGEMENTS

The authors would like to thank Gérard Jarry and Sylvie Huet for technical assistance.

Appendix -Supplementary data

Supplementary data associated with this article can be found online at…

REFERENCES

.

Ahlinder, L., B. Ekstrand-Hammarstrom, P. Geladi & L. Osterlund (2013) Large uptake of titania and iron oxide nanoparticles in the nucleus of lung epithelial cells as measured by Raman imaging and multivariate classification. *Biophys J,* 105**,** 310-9.

Aninat, C., A. Piton, D. Glaise, T. Le Charpentier, S. Langouët, F. Morel, C. Guguen-Guillouzo & A. Guillouzo (2006) Expression of cytochromes P450, conjugating enzymes and nuclear receptors in human hepatoma HepaRG cells. *Drug Metab Dispos,* 34**,** 75-83.

ANSES. 2017. Avis de l'Agence nationale de sécurité sanitaire de l'alimentation, de l'environnement et du travail, relatif à une demande d'avis relatif à l'exposition alimentaire aux nanoparticules de dioxyde de titane. https://www.anses.fr/fr/system/files/ERCA2017SA0020.pdf.

Azqueta, A. & M. Dusinska (2015) The use of the comet assay for the evaluation of the genotoxicity of nanomaterials. *Front Genet,* 6**,** 239.

Bermejo-Nogales, A., M. Connolly, P. Rosenkranz, M. L. Fernandez-Cruz & J. M. Navas (2017) Negligible cytotoxicity induced by different titanium dioxide nanoparticles in fish cell lines. *Ecotoxicol Environ Saf,* 138**,** 309-319.

Bessa, M. J., C. Costa, J. Reinosa, C. Pereira, S. Fraga, J. Fernandez, M. A. Banares & J. P. Teixeira (2017) Moving into advanced nanomaterials. Toxicity of rutile TiO2 nanoparticles immobilized in nanokaolin nanocomposites on HepG2 cell line. *Toxicol Appl Pharmacol,* 316**,** 114-122.

Bettini, S., E. Boutet-Robinet, C. Cartier, C. Comera, E. Gaultier, J. Dupuy, N. Naud, S. Tache, P. Grysan, S. Reguer, N. Thieriet, M. Refregiers, D. Thiaudiere, J. P. Cravedi, M. Carriere, J. N. Audinot, F. H. Pierre, L. Guzylack-Piriou & E. Houdeau (2017) Food-grade TiO2 impairs intestinal and systemic immune homeostasis, initiates preneoplastic lesions and promotes aberrant crypt development in the rat colon. *Sci Rep,* 7**,** 40373.

Brun, E., F. Barreau, G. Veronesi, B. Fayard, S. Sorieul, C. Chanéac, C. Carapito, T. Rabilloud, A. Mabondzo, N. Herlin-Boime & M. Carrière (2014) Titanium dioxide nanoparticle impact and translocation through ex vivo, in vivo and in vitro gut epithelia. *Part Fibre Toxicol.*, 25, 11:13.

Cabellos, J., C. Delpivo, E. Fernández-Rosas, S. Vázquez-Campos & G. Janer (2017) Contribution of M-cells and other experimental variables in the translocation of TiO2 nanoparticles across in vitro intestinal models. *NanoImpact*, 5, 51-60.

Chaudhry, Q., M. Scotter, J. Blackburn, B. Ross, A. Boxall, L. Castle, R. Aitken & R. Watkins (2008) Applications and implications of nanotechnologies for the food sector. *Food Addit Contam Part A Chem Anal Control Expo Risk Assess,* 25**,** 241-58.

Chen, H., R. Zhao, B. Wang, C. Cai, L. Zheng, H. Wang, M. Wang, H. Ouyang, X. Zhou, Z. Chai, Y. Zhao & W. Feng (2017) The effects of orally administered Ag, TiO2 and SiO2 nanoparticles on gut microbiota composition and colitis induction in mice. *NanoImpact*, 8, 80-88.

Chen, Z., Y. Wang, T. Ba, Y. Li, J. Pu, T. Chen, Y. Song, Y. Gu, Q. Qian, J. Yang & G. Jia (2014) Genotoxic evaluation of titanium dioxide nanoparticles in vivo and in vitro. *Toxicol Lett,* 226**,** 314-9.

Chong, M. N., B. Jin, C. W. Chow & C. Saint (2010) Recent developments in photocatalytic water treatment technology: a review. *Water Res,* 44**,** 2997-3027.

Collins, A. R., S. J. Duthie & V. L. Dobson (1993) Direct enzymic detection of endogenous oxidative base damage in human lymphocyte DNA. *Carcinogenesis,* 14**,** 1733-5.

Corradi, S., L. Gonzalez, L. C. Thomassen, D. Bilanicova, R. K. Birkedal, G. Pojana, A. Marcomini, K. A. Jensen, L. Leyns & M. Kirsch-Volders (2012) Influence of serum on in situ proliferation and genotoxicity in A549 human lung cells exposed to nanomaterials. *Mutat Res,* 745**,** 21-7.

Cui, Y., H. Liu, M. Zhou, Y. Duan, N. Li, X. Gong, R. Hu, M. Hong & F. Hong (2011) Signaling pathway of inflammatory responses in the mouse liver caused by TiO2 nanoparticles. *J Biomed Mater Res A,* 96**,** 221-9.

Di Bucchianico, S., F. Cappellini, F. Le Bihanic, Y. Zhang, K. Dreij & H. L. Karlsson (2016) Genotoxicity of TiO2 nanoparticles assessed by mini-gel comet assay and micronucleus scoring with flow cytometry. *Mutagenesis,* 32**,** 127–137.

Doak, S. H., S. M. Griffiths, B. Manshian, N. Singh, P. M. Williams, A. P. Brown & G. J. Jenkins (2009) Confounding experimental considerations in nanogenotoxicology. *Mutagenesis,* 24**,** 285-93.

Donner, E. M., A. Myhre, S. C. Brown, R. Boatman & D. B. Warheit (2016) In†vivo micronucleus studies with 6 titanium dioxide materials (3†pigment-grade & 3 nanoscale) in orally-exposed rats. *Regul Toxicol Pharmacol,* 74**,** 64-74.

Dorier, M., D. Beal, C. Marie-Desvergne, M. Dubosson, F. Barreau, E. Houdeau, N. Herlin-Boime & M. Carriere (2017) Continuous in vitro exposure of intestinal epithelial cells to E171 food additive causes oxidative stress, inducing oxidation of DNA bases but no endoplasmic reticulum stress. *Nanotoxicology,* 11**,** 751-761.

Dorier, M., E. Brun, G. Veronesi, F. Barreau, K. Pernet-Gallay, C. Desvergne, T. Rabilloud, C. Carapito, N. Herlin-Boime & M. Carriere (2015) Impact of anatase and rutile titanium dioxide nanoparticles on uptake carriers and efflux pumps in Caco-2 gut epithelial cells. *Nanoscale,* 7**,** 7352-60.

Dudefoi, W., K. Moniz, E. Allen-Vercoe, M.H. Ropers & V.K. Walker (2017) Impact of food grade and nano-TiO2 particles on a human intestinal community. *Food Chem Toxicol.*, 106(Pt A), 242-249.

Dusïnská, M. & A. Collins (1996) Detection of Oxidised Purines and UV Induced Photoproducts in DNA of Single Cells, by Inclusion of Lesionspecific Enzymes in the Comet Assay. *Alternatives Laboratory Animals,* 24**,** 405-411.

EFSA. 2016. Re-evaluation of titanium dioxide (E 171) as a food additive. doi: 10.2903/j.efsa.2016.4545: http://onlinelibrary.wiley.com/doi/10.2903/j.efsa.2016.4545/epdf.

El Yamani, N., A. R. Collins, E. Runden-Pran, L. M. Fjellsbo, S. Shaposhnikov, S. Zienolddiny & M. Dusinska (2017) In vitro genotoxicity testing of four reference metal nanomaterials, titanium dioxide, zinc oxide, cerium oxide and silver: towards reliable hazard assessment. *Mutagenesis,* 32**,** 117-126.

Farcal, L., F. Torres Andon, L. Di Cristo, B. M. Rotoli, O. Bussolati, E. Bergamaschi, A. Mech, N. B. Hartmann, K. Rasmussen, J. Riego-Sintes, J. Ponti, A. Kinsner-Ovaskainen, F. Rossi, A. Oomen, P. Bos, R. Chen, R. Bai, C. Chen, L. Rocks, N. Fulton, B. Ross, G. Hutchison, L. Tran, S. Mues, R. Ossig, J. Schnekenburger, L. Campagnolo, L. Vecchione, A. Pietroiusti & B. Fadeel (2015) Comprehensive In Vitro Toxicity Testing of a Panel of Representative Oxide Nanomaterials: First Steps towards an Intelligent Testing Strategy. *PLoS One,* 10**,** e0127174.

Ferraro, D., U. Anselmi-Tamburini, I. G. Tredici, V. Ricci & P. Sommi (2016) Overestimation of nanoparticles-induced DNA damage determined by the comet assay. *Nanotoxicology,* 10**,** 861-70.

Fisichella, M., F. Berenguer, G. Steinmetz, M. Auffan, J. Rose & O. Prat (2012) Intestinal toxicity evaluation of TiO2 degraded surface-treated nanoparticles: a combined physico-chemical and toxicogenomics approach in caco-2 cells. *Part Fibre Toxicol,* 9**,** 18.

George, J. M., M. Magogotya, M. A. Vetten, A. V. Buys & M. Gulumian (2017) From the Cover: An Investigation of the Genotoxicity and Interference of Gold Nanoparticles in Commonly Used In Vitro Mutagenicity and Genotoxicity Assays. *Toxicol Sci,* 156**,** 149-166.

Gerloff, K., I. Fenoglio, E. Carella, J. Kolling, C. Albrecht, A. W. Boots, I. Forster & R. P. Schins (2012) Distinctive toxicity of TiO2 rutile/anatase mixed phase nanoparticles on Caco-2 cells. *Chem Res Toxicol,* 25**,** 646-55.

Ghosh, M., D. Oner, R. C. Duca, S. M. Cokic, S. Seys, S. Kerkhofs, K. Van Landuyt, P. Hoet & L. Godderis (2017) Cyto-genotoxic and DNA methylation changes induced by different crystal phases of TiO2-np in bronchial epithelial (16-HBE) cells. *Mutat Res,* 796**,** 1-12.

Grissa, I., J. Elghoul, L. Ezzi, S. Chakroun, E. Kerkeni, M. Hassine, L. El Mir, M. Mehdi, H. Ben Cheikh & Z. Haouas (2015) Anemia and genotoxicity induced by sub-chronic intragastric treatment of rats with titanium dioxide nanoparticles. *Mutat Res Genet Toxicol Environ Mutagen,* 794**,** 25-31.

Guichard, Y., J. Schmit, C. Darne, L. Gate, M. Goutet, D. Rousset, O. Rastoix, R. Wrobel, O. Witschger, A. Martin, V. Fierro & S. Binet (2012) Cytotoxicity and genotoxicity of nanosized and microsized titanium dioxide and iron oxide particles in Syrian hamster embryo cells. *Ann Occup Hyg,* 56**,** 631-44.

Guo, Z., N.J. Martucci, F. Moreno-Olivas, E. Tako & G.J.Mahler (2017) Titanium Dioxide Nanoparticle Ingestion Alters Nutrient Absorption in an In Vitro Model of the Small Intestine. *NanoImpact*, 5, 70-82

Hamzeh, M. & G. I. Sunahara (2013) In vitro cytotoxicity and genotoxicity studies of titanium dioxide (TiO2) nanoparticles in Chinese hamster lung fibroblast cells. *Toxicol In Vitro,* 27**,** 864-73.

Hartmann, N. B., K. A. Jensen, A. Baun, K. Rasmussen, H. Rauscher, R. Tantra, D. Cupi, D. Gilliland, F. Pianella & J. M. Riego Sintes (2015) Techniques and Protocols for Dispersing Nanoparticle Powders in Aqueous Media-Is there a Rationale for Harmonization. *J Toxicol Environ Health B Crit Rev,* 18**,** 299-326.

Heringa, M. B., L. Geraets, J. C. van Eijkeren, R. J. Vandebriel, W. H. de Jong & A. G. Oomen (2016) Risk assessment of titanium dioxide nanoparticles via oral exposure, including toxicokinetic considerations. *Nanotoxicology,* 10**,** 1515-1525.

IARC. 2010. Monographs on the Evaluation of Carcinogenic Risks to Humans, VOLUME 93 : Carbon Black, Titanium Dioxide, and Talc 466. http://monographs.iarc.fr/ENG/Monographs/vol93/mono93.pdf.

Jin, C., Y. Tang, F. G. Yang, X. L. Li, S. Xu, X. Y. Fan, Y. Y. Huang & Y. J. Yang (2011) Cellular toxicity of TiO2 nanoparticles in anatase and rutile crystal phase. *Biol Trace Elem Res,* 141**,** 3-15.

Josse, R., C. Aninat, D. Glaise, J. Dumont, V. Fessard, F. Morel, J. M. Poul, C. Guguen-Guillouzo & A. Guillouzo (2008) Long-term functional stability of human HepaRG hepatocytes and use for chronic toxicity and genotoxicity studies. *Drug Metab Dispos,* 36**,** 1111-8.

Jugan, M. L., S. Barillet, A. Simon-Deckers, N. Herlin-Boime, S. Sauvaigo, T. Douki & M. Carriere (2012) Titanium dioxide nanoparticles exhibit genotoxicity and impair DNA repair activity in A549 cells. *Nanotoxicology,* 6**,** 501-13.

Jugan, M. L., S. Barillet, A. Simon-Deckers, S. Sauvaigo, T. Douki, N. Herlin & M. Carriere (2011) Cytotoxic and genotoxic impact of TiO2 nanoparticles on A549 cells. *J Biomed Nanotechnol,* 7**,** 22-3.

Kansara, K., P. Patel, D. Shah, R. K. Shukla, S. Singh, A. Kumar & A. Dhawan (2015) TiO2 nanoparticles induce DNA double strand breaks and cell cycle arrest in human alveolar cells. *Environ Mol Mutagen,* 56**,** 204-17.

Karlsson, H. L., S. Di Bucchianico, A. R. Collins & M. Dusinska (2015) Can the comet assay be used reliably to detect nanoparticle-induced genotoxicity? *Environ Mol Mutagen,* 56**,** 82-96.

Kermanizadeh, A., B. K. Gaiser, G. R. Hutchison & V. Stone (2012) An in vitro liver model--assessing oxidative stress and genotoxicity following exposure of hepatocytes to a panel of engineered nanomaterials. *Part Fibre Toxicol,* 9**,** 28.

Kermanizadeh, A., M. Lohr, M. Roursgaard, S. Messner, P. Gunness, J. M. Kelm, P. Moller, V. Stone & S. Loft (2014) Hepatic toxicology following single and multiple exposure of engineered nanomaterials utilising a novel primary human 3D liver microtissue model. *Part Fibre Toxicol,* 11**,** 56.

Kermanizadeh, A., G. Pojana, B. K. Gaiser, R. Birkedal, D. Bilanicova, H. Wallin, K. A. Jensen, B. Sellergren, G. R. Hutchison, A. Marcomini & V. Stone (2013) In vitro assessment of engineered nanomaterials using a hepatocyte cell line: cytotoxicity, pro-inflammatory cytokines and functional markers. *Nanotoxicology,* 7**,** 301-13.

Kim, J. A., C. Aberg, A. Salvati & K. A. Dawson (2011) Role of cell cycle on the cellular uptake and dilution of nanoparticles in a cell population. *Nat Nanotechnol,* 7**,** 62-8.

Le Hegarat, L., S. Huet & V. Fessard (2012) A co-culture system of human intestinal Caco-2 cells and lymphoblastoid TK6 cells for investigating the genotoxicity of oral compounds. *Mutagenesis,* 27**,** 631-6.

Li, Y., S. H. Doak, J. Yan, D. H. Chen, M. Zhou, R. A. Mittelstaedt, Y. Chen, C. Li & T. Chen (2017) Factors affecting the in vitro micronucleus assay for evaluation of nanomaterials. *Mutagenesis,* 32**,** 151-159.

Lim, J. H., P. Sisco, T. K. Mudalige, G. Sanchez-Pomales, P. C. Howard & S. W. Linder (2015) Detection and characterization of SiO2 and TiO2 nanostructures in dietary supplements. *J Agric Food Chem,* 63**,** 3144-52.

Magdolenova, Z., A. Collins, A. Kumar, A. Dhawan, V. Stone & M. Dusinska (2014) Mechanisms of genotoxicity. A review of in vitro and in vivo studies with engineered nanoparticles. *Nanotoxicology,* 8**,** 233-78.

McClements, D.J., G. DeLoid, G. Pyrgiotakis, J.A. Shatkin, H. Xiao & P. Demokritou (2016) The role of the food matrix and gastrointestinal tract in the assessment of biological properties of ingested engineered nanomaterials (iENMs): State of the science and knowledge gaps. *NanoImpact*, 3-4, 47-57,

Murdock, R. C., L. Braydich-Stolle, A. M. Schrand, J. J. Schlager & S. M. Hussain (2008) Characterization of nanomaterial dispersion in solution prior to in vitro exposure using dynamic light scattering technique. *Toxicol Sci,* 101**,** 239-53.

Nanogenotox. 2012a. D4.5: Surface charge, hydrodynamic size and size distributions by zetametry, dynamic light scattering (DLS) and small-angle X-ray scattering (SAXS) in optimized aqueous suspensions for titanium and silicon dioxide. https://www.anses.fr/en/system/files/nanogenotox_deliverable.5.pdf.

Nanogenotox. 2012b. WP 4 : Physicochemical Characterisation of Manufactured Nanomaterials (MNs) and Exposure Media (EMs), Deliverable 4.5: Nanomaterial datasets with requested physicochemical properties, Surface charge, hydrodynamic size and size distributions by zetametry, dynamic light scattering (DLS) and small-angle Xray scattering (SAXS) in optimum aqueous suspensions for titanium and silicon dioxide. https://www.anses.fr/en/system/files/nanogenotox_deliverable.5.pdf.

Nanogenotox. 2012c. D4.2: Transmission electron microscopic characterization of NANOGENOTOX nanomaterials, Key intrinsic physicochemical characteristics of NANOGENOTOX nanomaterials. http://www.oecd.org/officialdocuments/publicdisplaydocumentpdf/?cote=ENV/JM/MONO(2015)17/ANN4&docLanguage=En.

Nanogenotox. 2013b. WP5 : Towards a method for detecting the potential genotoxicity of nanomaterials, Deliverable 5: In vitro testing strategy for nanomaterials including database. https://www.anses.fr/en/system/files/nanogenotox_deliverable_6.pdf.

NANoREG. 2016. D2.08 SOP 02 For measurement of hydrodynamic Size-Distribution and Dispersion Stability by DLS. NANoREG: http://rivm.nl/en/About_RIVM/Mission_and_strategy/International_Affairs/International_Projects/Completed/NANoREG/deliverables:s_ezJOgJTEaL0lCqO1cAJQ/NANoREG_D2_08_SOP_02_For_measurement_of_hydrodynamic_Size_Distribution_and_Dispersion_Stability_by_DLS.org.

Numano, T., J. Xu, M. Futakuchi, K. Fukamachi, D. B. Alexander, F. Furukawa, J. Kanno, A. Hirose, H. Tsuda & M. Suzui (2014) Comparative study of toxic effects of anatase and rutile type nanosized titanium dioxide particles in vivo and in vitro. *Asian Pac J Cancer Prev,* 15**,** 929-35.

Peters, R. J., G. van Bemmel, Z. Herrera-Rivera, H. P. Helsper, H. J. Marvin, S. Weigel, P. C. Tromp, A. G. Oomen, A. G. Rietveld & H. Bouwmeester (2014) Characterization of titanium dioxide

nanoparticles in food products: analytical methods to define nanoparticles. *J Agric Food Chem,* 62**,** 6285-93.

Petkovic, J., B. Zegura, M. Stevanovic, N. Drnovsek, D. Uskokovic, S. Novak & M. Filipic (2011) DNA damage and alterations in expression of DNA damage responsive genes induced by TiO2 nanoparticles in human hepatoma HepG2 cells. *Nanotoxicology,* 5**,** 341-53.

Prasad, R. Y., S. O. Simmons, M. G. Killius, R. M. Zucker, A. D. Kligerman, C. F. Blackman, R. C. Fry & D. M. Demarini (2014) Cellular interactions and biological responses to titanium dioxide nanoparticles in HepG2 and BEAS-2B cells: role of cell culture media. *Environ Mol Mutagen,* 55**,** 336-42.

Prasad, R. Y., K. Wallace, K. M. Daniel, A. H. Tennant, R. M. Zucker, J. Strickland, K. Dreher, A. D. Kligerman, C. F. Blackman & D. M. Demarini (2013) Effect of treatment media on the agglomeration of titanium dioxide nanoparticles: impact on genotoxicity, cellular interaction, and cell cycle. *ACS Nano,* 7**,** 1929-42.

Proquin, H., C. Rodriguez-Ibarra, C. G. Moonen, I. M. Urrutia Ortega, J. J. Briede, T. M. de Kok, H. van Loveren & Y. I. Chirino (2017) Titanium dioxide food additive (E171) induces ROS formation and genotoxicity: contribution of micro and nano-sized fractions. *Mutagenesis,* 32**,** 139-149.

Rasmussen, k., E. Verleysen, F. Van Steen, N. Van Doren & K. Alstrup Jensen. 2014. Titanium Dioxide, NM-100, NM-101, NM-102, NM-103, NM-104, NM-105: Characterisation and Physico-Chemical Properties. 10.2788/79554 https://ec.europa.eu/jrc/en/publication/eur-scientific-and-technical-research-reports/titanium-dioxide-nm-100-nm-101-nm-102-nm-103-nm-104-nm-105-characterisation-and-physico.

Regulation (ec) no 1272/2008 of the european parliament and of the council. 2008. Classification, labelling and packaging of substances and mixtures, amending and repealing Directives 67/548/EEC and 1999/45/EC, and amending Regulation (EC) No 1907/2006. Official Journal of the European Union: http://eur-lex.europa.eu/LexUriServ/LexUriServ.do?uri=OJ:L:2008:353:0001:1355:en:PDF.

Roszak, J., M. Stepnik, M. Nocun, M. Ferlinska, A. Smok-Pieniazek, J. Grobelny, E. Tomaszewska, W. Wasowicz & M. Cieslak (2013) A strategy for in vitro safety testing of nanotitania-modified textile products. *J Hazard Mater,* 256-257**,** 67-75.

Saita, M., K. Kobayashi, F. Yoshino, H. Hase, T. Nonami, K. Kimoto & M. C. Lee (2012) ESR investigation of ROS generated by H2O2 bleaching with TiO2 coated HAp. *Dent Mater J,* 31**,** 458-64.

Saquib, Q., A. A. Al-Khedhairy, M. A. Siddiqui, F. M. Abou-Tarboush, A. Azam & J. Musarrat (2012) Titanium dioxide nanoparticles induced cytotoxicity, oxidative stress and DNA damage in human amnion epithelial (WISH) cells. *Toxicol In Vitro,* 26**,** 351-61.

Shukla, R. K., A. Kumar, D. Gurbani, A. K. Pandey, S. Singh & A. Dhawan (2013) TiO(2) nanoparticles induce oxidative DNA damage and apoptosis in human liver cells. *Nanotoxicology,* 7**,** 48-60.

Shukla, R. K., A. Kumar, N. V. Vallabani, A. K. Pandey & A. Dhawan (2014) Titanium dioxide nanoparticle-induced oxidative stress triggers DNA damage and hepatic injury in mice. *Nanomedicine (Lond),* 9**,** 1423-34.

Shukla, R. K., V. Sharma, A. K. Pandey, S. Singh, S. Sultana & A. Dhawan (2011) ROS-mediated genotoxicity induced by titanium dioxide nanoparticles in human epidermal cells. *Toxicol In Vitro,* 25**,** 231-41.

Srivastava, R. K., Q. Rahman, M. P. Kashyap, A. K. Singh, G. Jain, S. Jahan, M. Lohani, M. Lantow & A. B. Pant (2013) Nano-titanium dioxide induces genotoxicity and apoptosis in human lung cancer cell line, A549. *Hum Exp Toxicol,* 32**,** 153-66.

Stoccoro, A., S. Di Bucchianico, F. Coppede, J. Ponti, C. Uboldi, M. Blosi, C. Delpivo, S. Ortelli, A. L. Costa & L. Migliore (2017) Multiple endpoints to evaluate pristine and remediated titanium dioxide nanoparticles genotoxicity in lung epithelial A549 cells. *Toxicol Lett,* 276**,** 48-61.

Sund, J., J. Palomaki, N. Ahonen, K. Savolainen, H. Alenius & A. Puustinen (2014) Phagocytosis of nano-sized titanium dioxide triggers changes in protein acetylation. *J Proteomics,* 108**,** 469-83.

Sweeney, S., D. Berhanu, P. Ruenraroengsak, A. J. Thorley, E. Valsami-Jones & T. D. Tetley (2015) Nano-titanium dioxide bioreactivity with human alveolar type-I-like epithelial cells: Investigating crystalline phase as a critical determinant. *Nanotoxicology,* 9**,** 482-92.

Sycheva, L. P., V. S. Zhurkov, V. V. Iurchenko, N. O. Daugel-Dauge, M. A. Kovalenko, E. K. Krivtsova & A. D. Durnev (2011) Investigation of genotoxic and cytotoxic effects of micro- and nanosized titanium dioxide in six organs of mice in vivo. *Mutat Res,* 726**,** 8-14.

Tavares, A. M., H. Louro, S. Antunes, S. Quarre, S. Simar, P. J. De Temmerman, E. Verleysen, J. Mast, K. A. Jensen, H. Norppa, F. Nesslany & M. J. Silva (2014) Genotoxicity evaluation of nanosized titanium dioxide, synthetic amorphous silica and multi-walled carbon nanotubes in human lymphocytes. *Toxicol In Vitro,* 28**,** 60-9.

Teubl, B. J., C. Schimpel, G. Leitinger, B. Bauer, E. Frohlich, A. Zimmer & E. Roblegg (2015) Interactions between nano-TiO2 and the oral cavity: impact of nanomaterial surface hydrophilicity/hydrophobicity. *J Hazard Mater,* 286**,** 298-305.

Theron, J., J. A. Walker & T. E. Cloete (2008) Nanotechnology and water treatment: applications and emerging opportunities. *Crit Rev Microbiol,* 34**,** 43-69.

Trouiller, B., R. Reliene, A. Westbrook, P. Solaimani & R. H. Schiestl (2009) Titanium dioxide nanoparticles induce DNA damage and genetic instability in vivo in mice. *Cancer Res,* 69**,** 8784-9.

Uboldi, C., P. Urban, D. Gilliland, E. Bajak, E. Valsami-Jones, J. Ponti & F. Rossi (2016) Role of the crystalline form of titanium dioxide nanoparticles: Rutile, and not anatase, induces toxic effects in Balb/3T3 mouse fibroblasts. *Toxicol In Vitro,* 31**,** 137-45.

Ursini, C. L., D. Cavallo, A. M. Fresegna, A. Ciervo, R. Maiello, P. Tassone, G. Buresti, S. Casciardi & S. Iavicoli (2014) Evaluation of cytotoxic, genotoxic and inflammatory response in human alveolar and bronchial epithelial cells exposed to titanium dioxide nanoparticles. *J Appl Toxicol,* 34**,** 1209-19.

Valdiglesias, V., C. Costa, V. Sharma, G. Kilic, E. Pasaro, J. P. Teixeira, A. Dhawan & B. Laffon (2013) Comparative study on effects of two different types of titanium dioxide nanoparticles on human neuronal cells. *Food Chem Toxicol,* 57**,** 352-61.

Vales, G., L. Rubio & R. Marcos (2015) Long-term exposures to low doses of titanium dioxide nanoparticles induce cell transformation, but not genotoxic damage in BEAS-2B cells. *Nanotoxicology,* 9**,** 568-78.

Wang, J., G. Zhou, C. Chen, H. Yu, T. Wang, Y. Ma, G. Jia, Y. Gao, B. Li, J. Sun, Y. Li, F. Jiao, Y. Zhao & Z. Chai (2007) Acute toxicity and biodistribution of different sized titanium dioxide particles in mice after oral administration. *Toxicol Lett,* 168**,** 176-85.

Weir, A., P. Westerhoff, L. Fabricius, K. Hristovski & N. von Goetz (2012) Titanium dioxide nanoparticles in food and personal care products. *Environ Sci Technol,* 46**,** 2242-50.

Youssef, A. M., S. M. El-Sayed, H. H. Salama, H. S. El-Sayed & A. Dufresne (2015) Evaluation of bionanocomposites as packaging material on properties of soft white cheese during storage period. *Carbohydr Polym,* 132**,** 274-85.

Zhang, J., W. Song, J. Guo, J. Zhang, Z. Sun, L. Li, F. Ding & M. Gao (2013) Cytotoxicity of different sized TiO2 nanoparticles in mouse macrophages. *Toxicol Ind Health,* 29**,** 523-33.

Zijno, A., I. De Angelis, B. De Berardis, C. Andreoli, M. T. Russo, D. Pietraforte, G. Scorza, P. Degan, J. Ponti, F. Rossi & F. Barone (2015) Different mechanisms are involved in oxidative DNA damage and genotoxicity induction by ZnO and TiO2 nanoparticles in human colon carcinoma cells. *Toxicol In Vitro,* 29**,** 1503-12.

TABLES

Table 1: NM103 and NM104 characteristics from the JRC report.

NM code/JRC code	crystallite size[a]	Average particle[b] size	SSA[c]	Main elemental impurities[d]	Other information
NM 103 JRCNM1003a	23 nm	25 nm	51 m^2/g	Al, Si, Na, S	Rutile, thermal, hydrophobic, Al-coated
NM 104 JRCNM1004a	23 nm	25 nm	52/56 m^2/g	Al, Si, Na, S, Ca	Rutile, thermal, hydrophilic, Al-coated

[a]Crystal size was assessed by X-Ray-Diffraction (XRD)

[b]Average particle size was determined by TEM

[c]Average specific surface area (SSA) was determined by BET (Brunauer-Emmet-Teller)

[d]Impurities was performed by Inductively Coupled Plasma Optical Emission Spectrometry (ICP-OES)

Supplementary information available in the JRC report (Rasmussen et al. 2014) and in NANOGENOTOX reports (Nanogenotox 2012a, Nanogenotox 2012b, Nanogenotox 2012c).

Table 2: Equivalence between NM concentration in µg/ml and in µg/cm^2

Plate Format	**6-well**	**12-well**	**24-well**	**96-well**
Volume in well	2,5 ml	1 ml	0,5 ml	100µl
Surface area (cm^2)	9,5	3,8	1,9	0,32
µg/ml	**µg/cm^2**			
256	67,4	67,4	67,4	80
128	33,6	33,6	33,6	40
85	22,3	22,3	22,3	26,5
64	16.8	16.8	16.8	20
32	8.4	8.4	8.4	10
28	7,4	7,4	7,4	8,75
16	4.2	4.2	4.2	5
9	2,4	2,4	2,4	2,8
8	2.1	2.1	2.1	2.5
4	1	1	1	1.25

Table 3: Size characterization of NM103 and NM104.

The hydrodynamic diameter, zeta potential, and polydispersity index (PDI were determined by DLS (z-Ave) and NTA (mode) in the dispersion solution and treatment media (0h and 24h) at 100 µg/ml. Three or five independent experiments were performed. Data are presented as mean ± SD.

Sample (100 µg/ml)	PDI	Z-Ave (d.nm)	mode NTA (nm)	Zeta potential (mV)	PDI	Z-Ave (d.nm)	mode NTA (nm)	Zeta potential (mV)
	Dispersion solution (0h)				Dispersion solution (24h)			
NM 103	0.21 ± 0,3 [a]	611 ± 185 [a]	135 ± 14 [a]	-23.3 ± 0.4[a]	0.11 ± 0.1 [a]	820 ± 250 [a]	162± 11 [a]	-23.7 ± 3.5[a]
NM 104	0.15 ± 0.03[b]	370 ± 66 [b]	155 ± 14 [b]	-24.3 ± 0.6[a]	0.14 ±0.04 [b]	528 ± 124 [b]	153 ± 4 [b]	-18.4 ± 0.6[a]
	Medium DMEM + 10 %FBS (0h)				Medium DMEM + 10 % FBS (24h)			
NM 103	0.25 ± 0.01 [a]	267 ± 8 [a]	113 ± 6 [a]	-15.7 ± 0.8 [a]	0.23 ± 0.021 [a]	264 ± 3 [a]	126 ± 10 [a]	-15.7 ± 0.5 [a]
NM 104	0.18 ± 0.02 [b]	237 ± 6 [b]	121 ± 7 [b]	-15.8 ± 0.6 [a]	0.16 ± 0.04 [b]	249 ± 7 [b]	111 ± 9 [b]	-15.6 ± 0.9 [a]
	Medium William's + 5 % FBS (0h)				Medium William's + 5 % FBS (24h)			
NM 103	0.19 ± 0.1 [a]	270 ± 10 [a]	122 ± 8 [a]	-15.8 ± 0.4 [a]	0.24 ± 0.01 [a]	250 ± 10 [a]	131 ± 10 [a]	-15.9 ± 0.4 [a]
NM 104	0.18 ± 0.01 [a]	235 ± 4 [a]	117 ± 10 [a]	-15.5 ± 0.5 [a]	0.19 ± 0.01 [a]	240 ± 5 [a]	145 ± 9 [a]	-15.0 ± 0.7 [a]

[a] three independent experiments

[b] five independent experiments

Table 4: Micronuclei detection in Caco-2 and HepaRG cells treated with NM103 and NM104 TiO_2 NMs for 24h.

		NM 103						NM 104					MMS
Concentration ($\mu g/cm^2$)		0	**2**	**7**	**22**	**33**	**67**	**2**	**7**	**22**	**33**	**67**	**25 or 30 µg/ml**
HepaRG	%MNBN ±SEM	3.1 ± 0.1	2.3 ± 0.1	3 ± 0.2	2.1 ± 0.3	1.6 ± 0.1	2.4 ± 0.1	2.3 ± 0.1	2.3 ± 0.2	2 ±0.2	2.6 ± 0.1	2.9± 0.3	23.9 ± 5.9***
	%BNMN ±SEM	3 ± 0.4	1.7 ± 0.3	2.7 ± 0.7	0.8 ± 0.2	0.8 ± 0.1	0.7 ± 0.1	1.2± 0.2	4 ± 0.5	3.6 ±0.9	2.4 ± 0.6	2.4± 0.5	4.9 ± 0.8
	%POL ±SEM	1.9 ± 0.6	1.7 ± 0.2	2.2 ± 0.4	2.1 ± 0.1	2.8 ± 0.4	2.5 ± 0.2	2 ± 0.3	2 ± 0.4	2.2 ±0.3	2.1 ± 0.5	3.5±0.4	2.4 ± 0.3
	RI	100	114.19	110.74	120.74	115.6	111.11	104.4	107.7	108.9	136	113.8	87.65
Caco-2	%MNBN ±SEM	3.9±0.4	3.8±0.7	3.5±0.5	3.4±0.4	4.2±0.6	4.4±0.9	3.5±0.9	4.3±0.5	3.6±0.7	4±07	2.9±0.4	11.9 ±1.0**
	%BNMN ±SEM	2.9±1.2	1.9±0.5	2.8±1.0	2.5±0.8	2.6±0.8	1.6±0.5	1.6±0.6	2.3±0.5	1.8±0.6	2.2±0.6	2.1±0.5	2.6 ±0.8
	%POL ±SEM	2.9±0.9	2.8±0.6	2.7±0.7	2.9±0.7	2.9±0.7	2.1±0.7	2±0.8	2.5±0.6	2.8±0.8	2.6±0.6	2.3±0.7	1.6 ±0.5
	RI	100	100.5	97.8	94.2	98.5	101.2	99	90.5	101	94.8	94.1	61.6

Cells were exposed to increasing concentrations (2–80 µg/cm^2) of NMs or positive control (MMS 25 µg/ml for Caco-2 cells and 30 µg/ml for HepaRG cells) for 24h. Results are presented as means ± SEM as a percentage of binucleated cells (BN), micronucleated binucleated cells (MNBN), micronucleated mononucleated cells (MNMN), polynucleated cells (POL), and replicative index (RI), n= 3. *P< 0.05, **P< 0.01, ***P< 0.001.

FIGURES AND LEGENDS

Fig 1: TEM images of differentiated Caco-2 and HepaRG cross sections showing the uptake of NM103 and NM104 at 67.4 µg/cm^2 (B, D, G, I) and 7.4 µg/cm^2 (C, E, H, F) after 24h. NM aggregates are mostly found free (open arrow), in vesicles (full arrow) or in vacuoles (notched arrows), scale bar 1 µm, N: nucleus.

Fig 2: NRU assay (A, B) and cell counts from HCA (C, D) for the evaluation of cytotoxicity in differentiated Caco-2 and HepaRG cells exposed to NM103 and NM104 TiO_2 NMs for 24h. Values are presented as the mean ± SEM of 3 independent experiments.

Fig 3: mBCl assay (A, B) and CellROX staining (C,D) for the evaluation of oxidative stress in differentiated Caco-2 and HepaRG cells treated with NM103 and NM104 TiO_2 or the positive controls buthionine sulfoximine (BSO 100 µM) and menadione (MEN 50 µM) for 24h (A, B) or 3h (C, D). Images show DAPI (blue) and ROS (red) detected with CellROX in differentiated HepaRG cells. Data are presented as the means ± SEM of 3 independent experiments. **p< 0.01. White bar = 100 µm

Fig 4: Effect of NM103 and NM104 on γH2AX levels in differentiated Caco-2 and HepaRG cells. Cells were treated for 24 h (A, B) or 3 h (C, D) with NMs or positive controls (MMS at 30 µg/ml for Caco-2 and 60 µg/ml for HepaRG after 24h treatment or MEN at 50 µM for Caco-2 and 25 µM for HepaRG after 3 h treatment). Images show DAPI staining (blue) and γH2AX (red) in differentiated HepaRG cells. Data are presented as the mean ± SEM of 3 (A, B, C) to 5 (D) independent experiments. *p< 0.05. white bar = 100 µm

Fig 5: Detection of NMs interfering with DNA migration in Caco-2 cells treated with 2.5 µg/ml MMS. NMs were added in LMP when cells are deposited on slides and compared with control (CTR = Cells deposited on the slide with LMP alone). Values are presented as the mean percentage ± SEM of 2 C independent experiments.

Fig 6: Evaluation of DNA damage by the Comet assay detecting DNA damage (Fpg-) and oxidative DNA damage (Fpg+) in differentiated Caco-2 and HepaRG cells treated with TiO_2 NM103, NM104 or 30 µg/ml MMS for 24h. Values are presented as the mean percentage ± SEM of 4 independent

experiments. *** and **** indicate significantly higher levels compared to controls corresponding to $P < 0,001$ and 0,0001 respectively.

Highlights

- Study of the *in vitro* genotoxicity of TiO_2 NMs, and interactions with assays.
- Investigation of two rutile TiO_2 nanoforms of similar size differing in surface coating .
- No cytotoxic effects (viability, apoptosis, oxidative stress) were observed following treatment with NM-103 and NM-104 at concentrations up to 80 µg/cm^2.
- No genotoxic effects were observed in γH2AX and comet assays following treatment of Caco-2 and HepaRG cells with TiO_2 NMs
- The micronucleus assay is not recommended for TiO_2 NMs due to uncertainty in scoring.

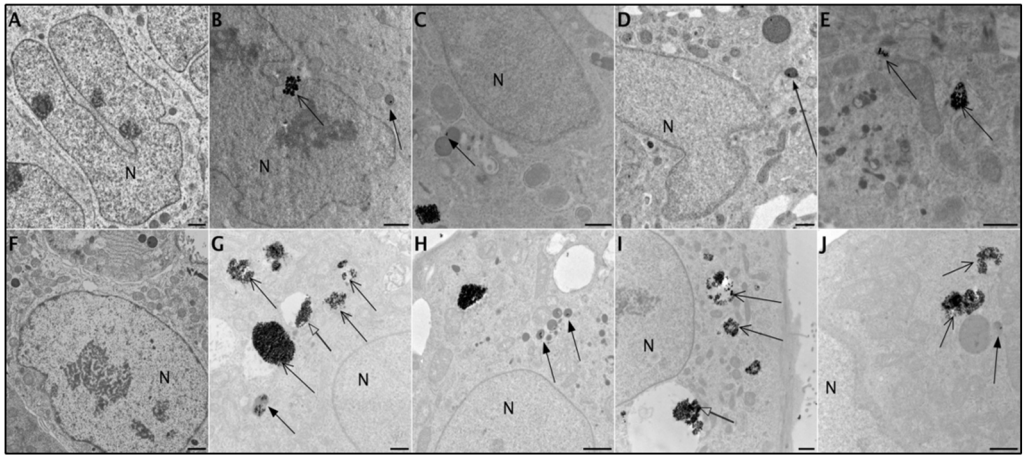

Figure 1

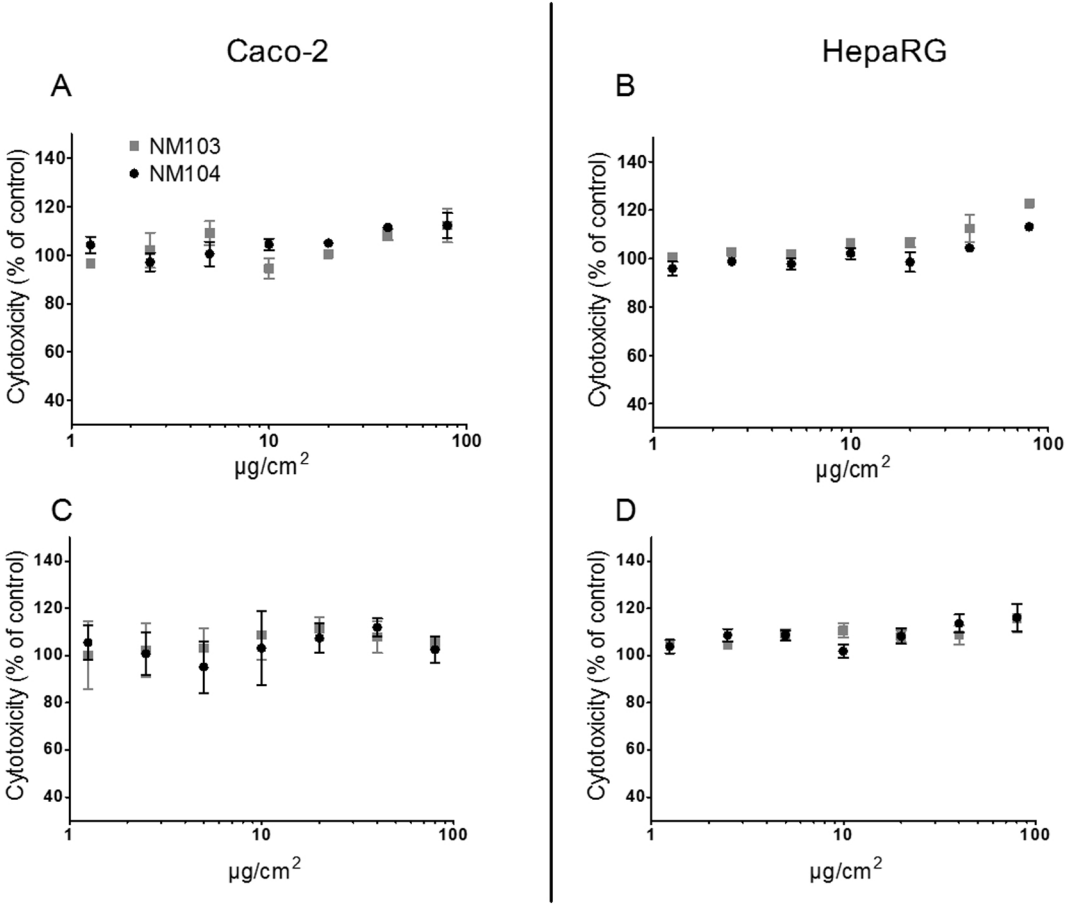
Caco-2
HepaRG
A
B
C
D
NM103
NM104
Cytotoxicity (% of control)
μg/cm2
140
120
100
80
60
40
1
10
100

Figure 2

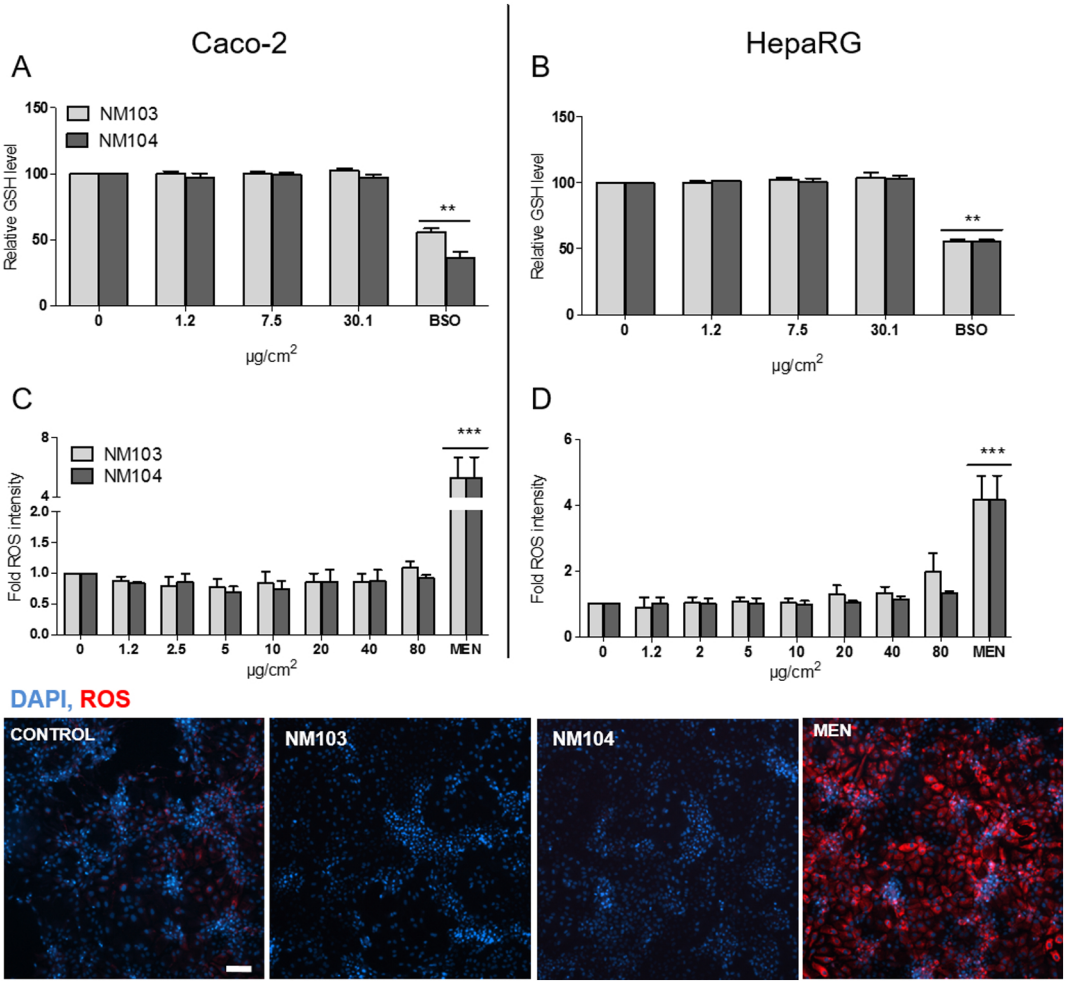
Caco-2
HepaRG
A
B
C
D
NM103
NM104
Relative GSH level
Fold ROS intensity
µg/cm2
0
1.2
2.5
5
7.5
10
20
30.1
40
80
BSO
MEN
**
***
DAPI, ROS
CONTROL
NM103
NM104
MEN

Figure 3

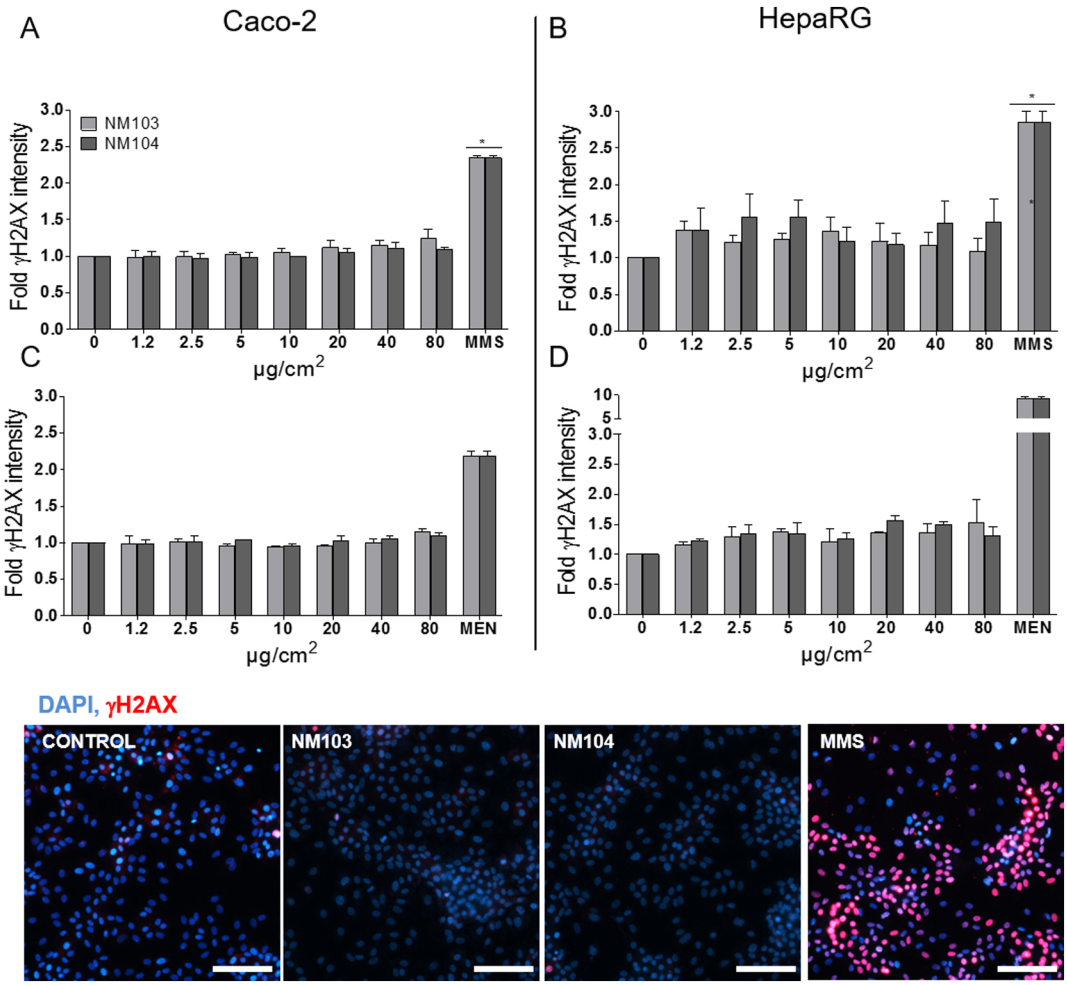
A
Caco-2
B
HepaRG
NM103
NM104
Fold γH2AX intensity
3.0
2.5
2.0
1.5
1.0
0.5
0.0
0
1.2
2.5
5
10
20
40
80
MMS
MEN
μg/cm2
*
C
D
10
5
DAPI, γH2AX
CONTROL
NM103
NM104
MMS

Figure 4

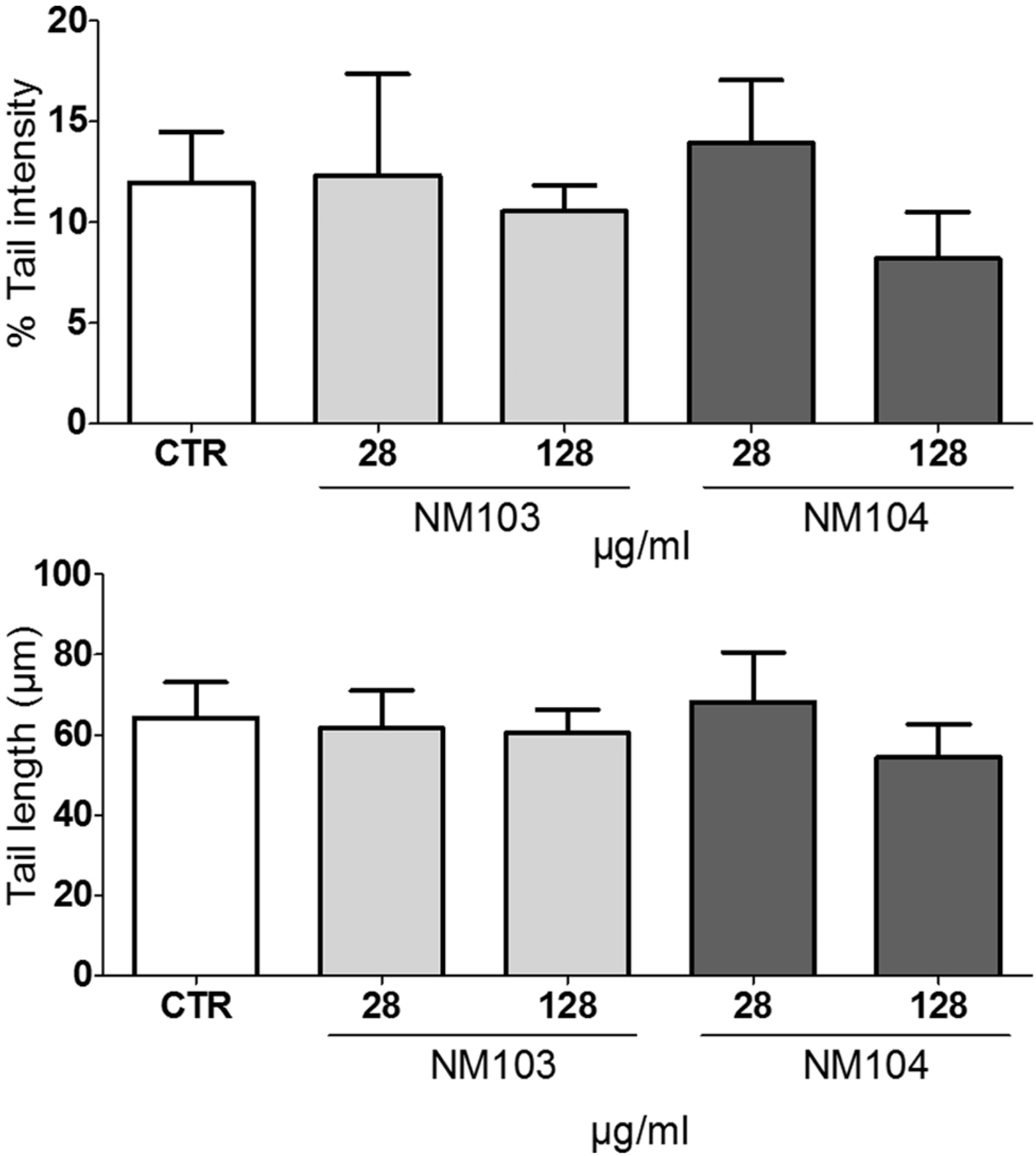
20
15
10
5
0
% Tail intensity
CTR
28
128
28
128
NM103
NM104
µg/ml
100
80
60
40
20
0
Tail length (µm)
CTR
28
128
28
128
NM103
NM104
µg/ml

Figure 5

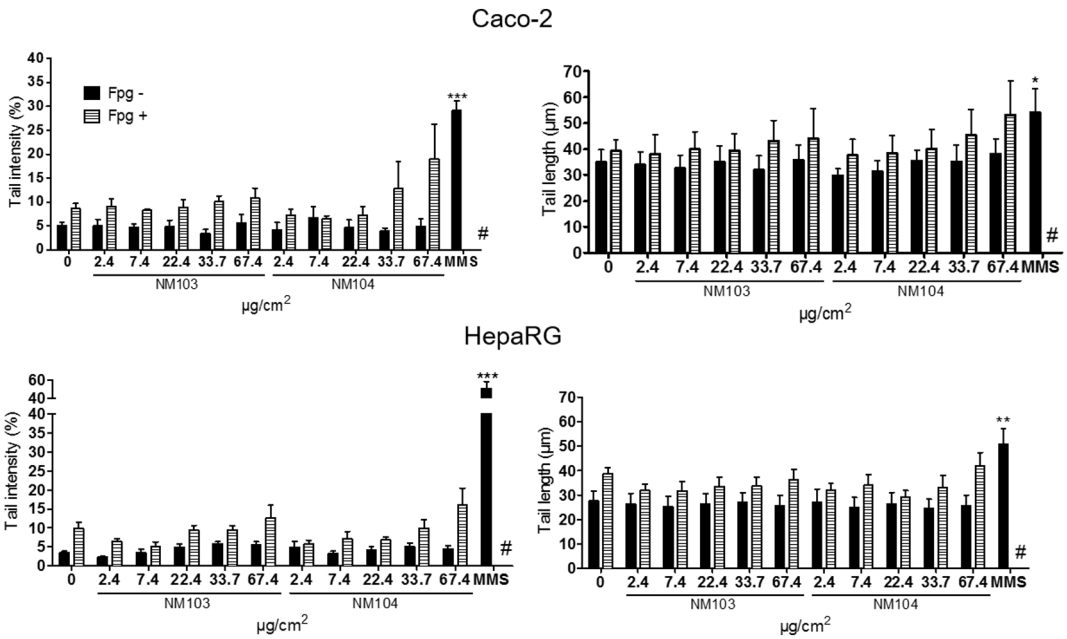
Caco-2
Fpg -
Fpg +
Tail intensity (%)
Tail length (µm)
***
*
#
0
2.4
7.4
22.4
33.7
67.4
MMS
NM103
NM104
µg/cm2
HepaRG
**

Figure 6